Ultrasound in Med. & Biol., Vol. 43, No. 12, pp. 2871–2881, 2017

0301-5629/$ - see front matter

https://doi.org/10.1016/j.ultrasmedbio.2017.08.005

● *Original Contribution*

PROTOCOL FOR ROBUST *IN VIVO* MEASUREMENTS OF ERYTHROCYTE AGGREGATION USING ULTRASOUND SPECTROSCOPY

Julian Garcia-Duitama,* Boris Chayer,* Damien Garcia,*,†,‡,§ Yves Goussard,¶,‖ and Guy Cloutier*,‡,§

* Laboratory of Biorheology and Medical Ultrasonics, University of Montreal Hospital Research Center (CRCHUM), Montreal, Quebec, Canada; † Research Unit of Biomechanics and Imaging in Cardiology, CRCHUM, Montreal, Quebec, Canada; ‡ Department of Radiology, Radio-oncology and Nuclear Medicine, University of Montreal, Montreal, Quebec, Canada; § Institute of Biomedical Engineering, University of Montreal, Montreal, Quebec, Canada; ¶ Department of Electrical Engineering, École Polytechnique of Montreal, Montreal, Quebec, Canada; and ‖ Institute of Biomedical Engineering, École Polytechnique of Montreal, Montreal, Quebec, Canada

(*Received* 27 *February* 2017; *revised* 19 *July* 2017; *in final form* 8 *August* 2017)

Abstract—Erythrocyte aggregation is a non-specific marker of acute and chronic inflammation. Although it is usual to evaluate this phenomenon from blood samples analyzed in laboratory instruments, *in vivo* real-time assessment of aggregation is possible with spectral ultrasound techniques. However, variable blood flow can affect the interpretation of acoustic measures. Therefore, flow standardization is required. Two techniques of flow standardization were evaluated with porcine and equine blood samples in Couette flow. These techniques consisted in either stopping the flow or reducing it. Then, the sensibility and repeatability of the retained method were evaluated in 11 human volunteers. We observed that stopping the flow compromised interpretation and repeatability. Conversely, maintaining a low flow provided repeatable measures and could distinguish between normal and high extents of erythrocyte aggregation. Agreement was observed between *in vivo* and *ex vivo* measures of the phenomenon (R^2 = 82.7%, p value < 0.0001). These results support the feasibility of assessing *in vivo* erythrocyte aggregation in humans by quantitative ultrasound means. (E-mail: guy.cloutier@umontreal.ca) © 2017 World Federation for Ultrasound in Medicine & Biology. All rights reserved.

Key Words: **Quantitative ultrasound, backscatter coefficient, spectral analysis, erythrocyte aggregation, flow phantom study, *in vivo* measures, reliability.**

INTRODUCTION

Erythrocyte aggregation refers to the reversible tendency of mammalian red blood cells (RBCs) to associate under low blood flow or stagnation conditions (Baskurt et al. 2011). RBC hyper-aggregation has been extensively reported in various pathophysiological conditions, such as cancers, diabetes mellitus and cardiovascular diseases. In particular, hyper-aggregation is often associated with inflammatory disorders, as some proteins released in the bloodstream, notably fibrinogen, enhance inter-RBC attraction forces (Weng et al. 1996a). Consequently, indicators of erythrocyte aggregation are commonly used in clinical research as a surrogate marker of inflammation (Berliner et al. 2005; Reggiori et al. 2009).

Several techniques have been proposed for the quantitative measurement of erythrocyte aggregation. In general, the measure relies on laboratory-based instruments requiring blood sampling and the use of anticoagulant. Indices based on erythrocyte sedimentation rate (Fåhraeus 1929), blood viscosity (Chien et al. 1967) or light transmission and scattering (Baskurt et al. 1998) are used as indicators of the degree of RBC aggregation. Particularly, the laser aggregometer is still the most accepted instrument for RBC aggregation measurements (Baskurt et al. 2009; Zhao et al. 1999). The key advantage of this instrument is that the measure is done under well-controlled conditions, thus reducing the effect of confounding factors (*i.e.,* shear rate, hematocrit, sedimentation and temperature).

In vivo assessment of RBC aggregation has also been proposed, mostly using ultrasound approaches (Rouffiac

Address correspondence to: Guy Cloutier, Research Center, University of Montreal Hospital; Viger Tower (Room R11-464); 900 rue Saint-Denis, Montréal, Québec, Canada, H2X 0A9. E-mail: guy.cloutier@umontreal.ca

et al. 2004; Tripette et al. 2013, 2015). The main aim of *in vivo* measurements is to continuously monitor the acute inflammation response in patients under critical care evaluation, notably those at risk of septicemia (Fernandes 2013; Tripette et al. 2013). The most used ultrasound technique is based on the measurement of a fundamental acoustic property of blood: the backscatter coefficient (BSC). The BSC is a quantitative value that reflects the capacity of a tissue to return acoustic energy at a certain frequency (Shung 2005). At any physiologic hematocrit, the BSC of blood increases in amplitude as a result of erythrocyte aggregation (Foster et al. 1994; Yu and Cloutier 2007; Yuan and Shung 1988). The main advantage of the BSC is that it is independent of the ultrasound system characteristics, so reported values can be compared between laboratories (Anderson et al. 2010). It is a common practice to summarize the frequency-dependent BSC with descriptive parameters, which is usually represented by a spectral curve fitted to scattering models (Franceschini et al. 2008; Yu and Cloutier 2007) or by taking the slope of the curve (Scheipers 2009). Other ultrasound techniques, such as power Doppler (Cloutier and Shung 1992) and envelope statistics (Destrempes et al. 2016), have also been proposed to quantify RBC aggregation.

Despite several efforts, there are still a few challenges for *in vivo* measurements by ultrasound. In contrast to laboratory-based *ex vivo* techniques, *in vivo* measurements imply a lack of control over factors such as the blood temperature, hematocrit and flow shear rate. Most authors implicitly consider that changes in body temperature are minimal and neglect this effect, which is acceptable under changes up to a few degrees Celsius (Baskurt et al. 2011; Neumann et al. 1987). On the other hand, hematocrit changes can cause significant differences in measurements and are usually corrected for or considered constant unless a hemorrhagic condition prevails.

The main confounding factor for *in vivo* assessment of RBC aggregation is the flow shear rate. Shearing forces are created by flowing blood traveling at different velocities depending on the position in the vessel. RBC aggregation typically occurs at shear rates between 0.0001 and 100 s^{-1}, with more aggregation present at the lowest range (Chien et al. 1967). In conditions such as diabetes mellitus, shear rates above 100 s^{-1} may be necessary to disrupt pathologic RBC aggregates (Cloutier et al. 2008). At high shears near the vessel wall, aggregates partially or totally dissociate (Fig. 1). Conversely, low shear rates can be found close to the longitudinal axis of a vessel or in recirculation zones, which enhance RBC aggregation.

A minimum shear rate is necessary to promote aggregation as collision efficiency between RBCs is reduced

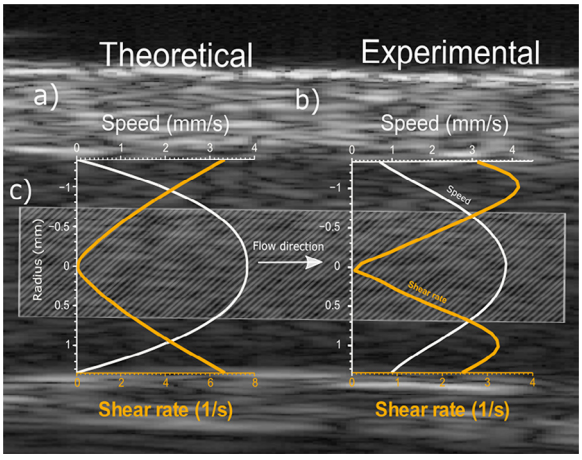

Fig. 1. Examples of *in vivo* velocity and shear rate profiles in vein flow. (a) Theory predicts a blunted parabolic velocity profile created by the non-Newtonian behavior of blood. Shear rate is zero at the central axis of the vein and maximum at the wall. (b) Experimental flow profile calculated with the particle image velocimetry method (see details below). Artifacts close to the wall are caused by the lack of precision of the estimation under 1 mm/s because of the use of a spatial filter. (c) Region of interest for spectral analysis (see details below). This area contains a median shear rate of about 3 s^{-1}.

under flow stagnation (Shehada et al. 1993). Flow pulsatility in arteries can also modulate the level of aggregation (Cloutier and Shung 1992; De Kroon et al. 1991). With *ex vivo* Couette systems made of concentric cylinders, as typically used in rheology studies, steady or pulsatile flow can be obtained and shearing forces can be precisely controlled. Couette devices allow the time course of RBC aggregation to be followed from a disaggregated state at a high shear rate (*i.e.*, at a high relative rotation speed of concentric cylinders), or permit evaluation of the impact of a specific shear rate on aggregate size (Nguyen et al. 2008).

Two approaches have been proposed for shear rate adjustment in *in vivo* RBC aggregation measures with ultrasound: either reducing the blood flow by clamping the vessel or no control at all (*i.e.*, natural flow). In porcine experiments (Rouffiac et al. 2004; Tripette et al. 2013), an adjustable clamp was applied downstream of the ultrasound transducer to reduce the blood flow. Low-velocity profiles could give a relatively narrow dispersion of shear rates. In those studies, ultrasound acquisitions were done during the first minute after stabilization of the flow. In human (Tripette et al. 2015) and rabbit (Yu et al. 2011) studies, the venous flow was not controlled, but the maximum velocity was measured to estimate the mean shear rate assuming Poiseuille flow.

The objective of this study was to describe an ultrasound protocol to assess the erythrocyte aggregation level *in vivo* that can be used in a clinical context.

This article describes the impact of reduced flow and flow stoppage on ultrasound measurements of RBC aggregation based on the BSC and its performance in detecting biological variability of the phenomenon. This study was divided into two stages: (i) evaluation and selection of shear-control methods *ex vivo* and (ii) *in vivo* evaluation of the shear-control method retained from the first stage.

METHODS

Blood preparation for ex vivo *experiments*

Five porcine and three equine blood samples of 500 mL were collected from slaughterhouses, as these species have levels of RBC aggregation close to normal and elevated abnormal levels as in humans, respectively (Weng et al. 1996b; Windberger et al. 2003). The samples were anticoagulated with 1.5 mg/mL ethylenediaminetetraacetic acid (EDTA) (Baskurt et al. 2009), stored at room temperature and used within 13 h of collection. To better simulate clinical measurement conditions, white blood cells and platelets were conserved, and the hematocrit was adjusted to 40% by adding/removing autologous plasma after 10 min of centrifugation at 1400*g* (3200 rpm). With the aim of degassing the sample, blood preparations were gently stirred for at least 15 min before ultrasound and laser aggregometry measurements.

Apparatus for ex vivo *assessment of erythrocyte aggregation*

Erythrocyte aggregation of all samples was assessed by laser aggregometry (Regulest, Florange, France). This method constitutes an accepted reference in hemorheological practice (Baskurt et al. 2009, 2011). This apparatus employs a Couette system to shear blood samples of 1 mL to disaggregate erythrocytes and, then, to monitor the intensity of scattered light as aggregates are formed during 2 min of monitoring. Aggregation indices at 10 and 60 s were measured, and are labeled S_{10} and S_{60}, respectively. Higher values of these indices indicate a higher level of RBC aggregation. All measurements were performed in a thermostatic chamber with blood samples pre-incubated at 37°C.

All *ex vivo* ultrasound experiments were conducted at room temperature in a self-designed Couette system. This instrument was not conceptualized to be used with a thermostatic chamber. The apparatus consists of two concentric cylinders 8 and 8.2 cm in radius, as detailed elsewhere (Nguyen et al. 2008). Approximately 100 mL of blood was placed in the 2-mm gap and subjected to the desired shear rate. An acoustic window with a cylindrical geometry was molded into the Couette system with agar gelatin at 2% in distilled water (w/w).

Ex vivo *ultrasound protocol*

The shearing protocol using the Couette system consisted of three consecutive stages: disaggregation, stabilization and ultrasound data acquisition (Fig. 2). During the disaggregation stage, an initial shear rate of 300 s^{-1} was applied to the blood for 10 s to induce the complete disaggregation of the erythrocytes. This shear rate is lower than that used by laser aggregometry and does not cause hemolysis of the sample (Arwatz and Smits 2013). During the stabilization stage, a pre-defined shear rate was applied for 30 s to simulate an *in vivo* pre-measuring flowing condition. The stabilization shears repeated in all experiments were 75, 50, 25, 10, 5 and 1 s^{-1} (Fig. 2 gives values of 75 and 25 s^{-1}). Then, during the acquisition stage, the two shear control methods were tested as follows. For stopped-flow experiments, the rotating cylinder of the Couette system was abruptly stopped. For residual flow experiments, the shear rate was suddenly changed to 5 s^{-1}. In both cases, the ultrasound acquisition started for 120 s, recording two frames per second.

In vivo *ultrasound protocol*

To validate the feasibility of the retained protocol in a clinical context, 11 volunteers between 22 and 52 y of age participated in this study. The protocol was approved by the human ethics committee of the University of Montreal Hospital Research Center. All volunteers provided a written informed consent for blood sampling and ultrasound data recording. No particular exclusion criteria were applied, as no group differentiation was intended

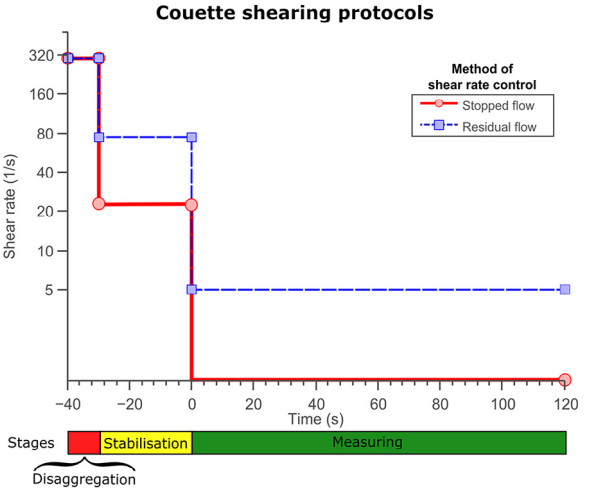

Fig. 2. Couette shearing protocol. During the disaggregation stage, blood was sheared at 300 s^{-1} to dissociate any aggregate. During the stabilization stage, blood was sheared at several transitional levels (shear rates of 75, 50, 25, 10, 5 and 1 s^{-1} were employed). During the measuring stage, ultrasound images were acquired for spectral analysis in post-processing.

for this study. In particular, two individuals declared to have a pro-aggregating disease of cardiovascular or metabolic origin (*i.e.*, aortic aneurysm and diabetes mellitus, respectively). The hematocrit was measured by microcentrifugation on EDTA-anticoagulated blood samples. The laser aggregometry method was used to measure parameters S_{10} and S_{60}.

Only the reduced flow protocol pre-tested *ex vivo* was retained as it turned out to be more repeatable. Ultrasound acquisitions were performed over the medial antebrachial vein of the left arm with subjects in the supine position and the arm in the resting horizontal position. Venous recordings were preferred over arterial ones to reduce the confounding impact of pulsatile flow. The ultrasound transducer was fixed to the arm using a support to produce a longitudinal view of the vein. Then, a hydraulic tourniquet was placed downstream of the transducer to control the flow velocity, increasing gradually the pressure until the desired shear rate was attained.

A median shear rate of 5 s^{-1} was targeted. However, pre-testing on a few volunteers did not always allow a high enough blood velocity to be attained to reach this value. A residual shear rate of 3 s^{-1} was then preferred. To estimate the median shear rate, it was necessary to obtain a velocity map. As Doppler ultrasound is not precise enough for the required speeds, we employed a particle image velocimetry (PIV) algorithm (Garcia 2011), as previously employed in the context of the present study (Garcia-Duitama et al. 2016). Briefly, the algorithm estimated a displacement map by phase correlation for each pair of radiofrequency (RF) images. Then, the displacements were divided by the frame rate to obtain an instantaneous velocity map. A spatial derivative of the radial velocity was used to obtain the instantaneous shear rate profile (see Fig. 1). The steadiness of the blood velocity and shear rate was monitored during data acquisition using the same PIV algorithm. Ultrasound data for BSC estimation were taken after 1 min of flow stabilization.

Evaluation of the variability and sensitivity of the in vivo *technique*

To evaluate the intra-assay variability of *in vivo* measurements, 10 repeated ultrasound measures were done on a single volunteer. Afterward, the coefficient of variation (CV) was computed for each ultrasound spectral parameter, as recommended in the guidelines of hemorheological techniques (Baskurt et al. 2009). Formally, $CV=\sigma/\mu$, where σ and μ represent the standard deviation and the mean value of repeated measures, respectively.

The sensitivity of the technique in detecting biological inter-subject variations in RBC aggregation was evaluated by correlating BSC parameters with the laser aggregometer indices S_{10} and S_{60}. The coefficient of determination (R^2) between the *in vivo* and *ex vivo* indices was calculated.

Ultrasound acquisitions

Ultrasound data were acquired with a high-frequency scanner (Model Vevo 770, VisualSonics, Toronto, ON, Canada) at an imaging rate of 26 frames/s. The scanner was equipped with an oscillatory single-element transducer (Model RMV-703), with a nominal central frequency of 35 MHz and a −15-dB bandwidth of 22.5–52.5 MHz. RF signals were amplified by a pulse receiver system (Model 5900 PR, Panametrics, Waltham, MA, USA) and digitized at 250 MHz by a 12-bit acquisition card (Model CS12501, GageScope, Montreal, QC, Canada). To follow the RBC aggregation kinetics, a waveform generator (Model 33250 A, Agilent, Santa Clara, CA, USA) triggered the recording of the first two frames at each second.

Regions of interest in ultrasound images

For *ex vivo* measurements in the Couette system, the region of interest (ROI) included the entire gap between the two cylinders. In this case, we assumed a homogeneous aggregation as the Couette system applies a constant shear rate in the entire sample. In contrast, for *in vivo* experiments, the ROI consisted of half of the lumen, going from one-fourth to three-fourths of the diameter in longitudinal view, thus avoiding the regions close to the walls at highest shear rates (Fig. 1c). ROIs were manually segmented in both *ex vivo* and *in vivo* images.

BSC estimation

The blood BSC was estimated using the reference phantom technique, as detailed in Garcia-Duitama et al. (2015). The reference medium consisted of a phosphate-buffered saline (PBS) solution of porcine erythrocytes at a volume concentration (*i.e.*, the hematocrit) of 4%. This medium constitutes a reproducible reference that can be modeled analytically, as it inhibits erythrocyte aggregation and presents reduced scattering interference (Wang and Shung 1997). For *ex vivo* experiments, this solution was sheared in the same Couette apparatus at 5 s^{-1} to acquire ultrasound reference data. For reference *in vivo* measures, the solution was placed in a plastic beaker in which the probe was immersed. To avoid sedimentation, it was gently agitated with a magnetic stirrer for 30 s and then stopped for 5 s before the acquisition.

The theoretical BSC of the reference medium, BSC_R, was analytically calculated using the adaptation of Franceschini et al. (2011):

$$BSC_R(f) = m \cdot \theta(f, s, \gamma_z) \cdot S(h, f, s) \quad (1)$$

In eqn (1), f is the insonification frequency; m is the number density of erythrocytes in the medium, corresponding to the hematocrit divided by the volume of a single erythrocyte; θ is the backscatter cross section of a single erythrocyte, as defined in Franceschini and Cloutier (2013); s is the radius of an erythrocyte; γ_z is the acoustic impedance contrast of an erythrocyte within the PBS solution; S is the structure function for rigid spheres (Wertheim 1963), which compensates in frequency the intercellular scattering interference, as applied in Garcia-Duitama et al. (2015); and h is the hematocrit.

The BSC spectral analysis was based on the 1-D power spectrum of the RF data in the ROI using the Welch (1967) method. For this, the RF image was split up with windows of 0.37 × 0.07 mm in the lateral and axial directions, respectively. Adjacent windows were overlapped by 50%. This technique allowed averaging of at least 220 windows per frame *in vivo* and more than a thousand windows *ex vivo*. For each segment, a Hann window was applied and its periodogram was computed. The average of the squared magnitude periodogram was considered the power spectrum of the window. Then, the BSC of the sample, BSC_S, was estimated using

$$BSC_S(f) = \frac{1}{|I|} \sum_{i \in I} \frac{S_S(i, f) 10^{\frac{2 \cdot \alpha_S \cdot d_i \cdot f}{10}}}{S_R(i, f) 10^{\frac{2 \cdot \alpha_R \cdot d_i \cdot f}{10}}} BSC_R(f) \quad (2)$$

where I is the collection of windows dividing the ROI, and $|\cdot|$ is the cardinality function (*i.e.*, it returns the number of elements of the parameter); S_S and S_R are the power spectra of a window i taken within the sample and the reference medium, respectively; α_S and α_R are the total ultrasound attenuation coefficients of the latter media, respectively; and d_i is the average depth of a window.

The speed of sound and attenuation coefficient of whole blood and of the erythrocyte reference solution was assumed to be 1580 m/s for both media (Bushberg et al. 2002), and 0.23 and 0.014 dB/cm/MHz, respectively (Wang and Shung 1997). The radius of a porcine erythrocyte was approximated to 2.34 µm as derived from the mean corpuscular volume of a spherical RBC of 54 fL (*i.e.*, 10^{-15} L) (Windberger et al. 2003). The acoustic impedance contrast of erythrocytes within PBS was estimated at 0.11 (Shung 1982). For *ex vivo* experiments, the attenuation of the agar gel coupling was estimated using a standard substitution method (Shung 2005). Agar attenuation was evaluated at 0.08 dB/cm/MHz. For *in vivo* measurements, the total attenuation coefficient was estimated using the spectral fit algorithm (Bigelow and O'Brien 2005). Briefly, this algorithm estimates simultaneously the BSC and the attenuation, assuming a Gaussian form factor for the BSC (Insana and Brown 1993). Note that we kept only the total attenuation coefficient of the spectral fit algorithm. The reference phantom required for this algorithm was the solution of erythrocytes in PBS at 4% hematocrit, as also employed during the BSC_R estimation.

Parameterization of the BSC

The BSC spectrum was estimated and parameterized by its log–log slope (*i.e.*, spectral slope) and by its amplitude at 25 MHz (named midband amplitude). The spectral slope was estimated by fitting to a line the BSC versus frequency in the whole useable bandwidth (*i.e.*, between 15 and 39 MHz) and keeping the slope of the line. A slope of 4 is indicative of Rayleigh scattering and corresponds to disaggregated RBCs (Shung et al. 1976).

RESULTS

Ex vivo *assessment of erythrocyte aggregation using laser aggregometry*

Equine blood had the highest levels of RBC aggregation after 10 and 60 s of aggregation, when evaluated by laser aggregometry (Table 1). On average, porcine RBC aggregation was higher than that of human subjects. The S_{10} index was in the same range as in other studies in the literature (Weng et al. 1996a, 1996b). This suggests that porcine blood and equine blood can be used as models of enhanced human RBC aggregation.

Considerations for evaluating RBC aggregation with ultrasound

When either stopping the flow or applying a residual shear rate, the RBC aggregation generally stabilized at a characteristic steady state within the 120 s of monitoring (Figs. 3 and 4). A rapid aggregation, characterized by enhanced midband amplitude or lower spectral slope, was observed in the first 10 to 20 s. In the analysis presented in the following sections, we consider the ultrasound parameters at the steady state (*i.e.*, at 120 s) to characterize the erythrocyte aggregation of a given blood sample.

Table 1. Averaged erythrocyte aggregation in three species as assessed by laser aggregometry*

	Human	Pig	Horse
S_{10} (no units)	21.8 ± 4.3	27.9 ± 3.9	32.3 ± 2.1
S_{60} (no units)	32.2 ± 3.0	34.2 ± 5.1	36.9 ± 2.4
Number of participants	11	5	3

* Parameters S_{10} and S_{60} represent the aggregometer measurements 10 and 60 s after cessation of shearing, respectively. Indices are expressed as the mean ± standard deviation.

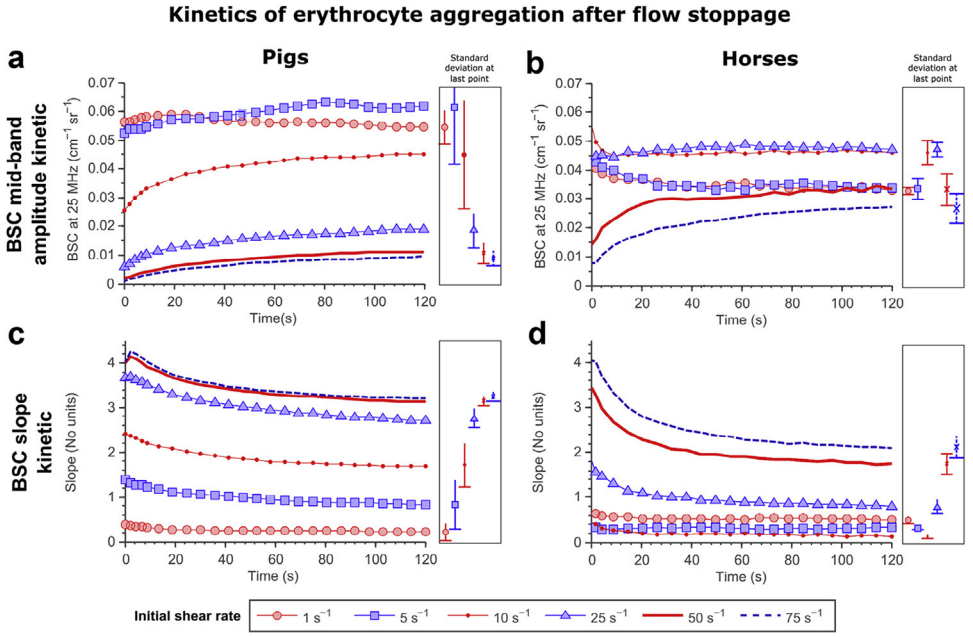

Fig. 3. Average kinetics of erythrocyte aggregation after flow stoppage, monitored by the midband amplitude (a, b) and by the spectral slope (c, d). Comparison of porcine (a, c) and equine (b, d) blood samples. By application of different initial shear rates, amplitude and slope of the backscattering coefficient do not converge to the same values. This causes a lack of repeatability for the flow stoppage technique.

Ex vivo *kinetics of RBC aggregation with stopped flow*

The stopped-flow technique lacked repeatability because the steady state of the BSC was dependent on the initial shear rate imposed by the Couette system (Fig. 3). Although there are certain exceptions, the midband amplitude at the steady state was inversely proportional to the initial shear rate, especially in the porcine case. On the contrary, the slope at steady state

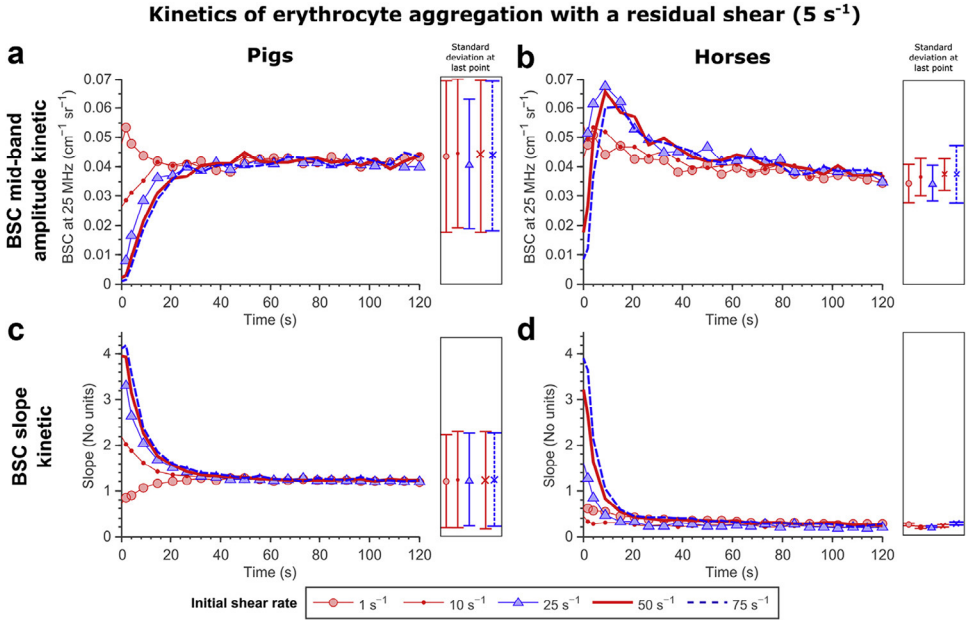

Fig. 4. Average kinetics of erythrocyte aggregation with a residual shear at 5 s^{-1}, monitored by the midband amplitude (a, b) and the spectral slope (c, d). Comparison of porcine (a, c) and equine (b, d) blood samples. The amplitude and slope of the backscattering coefficient converge to the same mean value whatever the initial shear rate applied. This suggests a better repeatability for this technique of shear rate control.

was proportional to the initial shear rate, although also with certain exceptions.

With porcine blood, the highest shear rates (*i.e.*, 75 and 50 s^{-1}) induced complete disaggregation at $t = 0$ s, as exemplified by the slope close to 4 and the midband amplitude close to zero (Fig. 3a, c). Conversely, with equine blood, a shear rate of 50 s^{-1} was insufficient to obtain the same level of disaggregation as at 75 s^{-1}, as reflected by the slope lower than 4 (Fig. 3b, d).

Ex vivo *kinetics of RBC aggregation with low flow*

When a residual shear rate of 5 s^{-1} was applied, the BSC of blood reached a reproducible steady state with a single midband amplitude and slope, independently of the initial state of aggregation (Fig. 4). However, RBC aggregation kinetics differed depending on the starting level of aggregation: high shear rates induced starting points at $t = 0$ s with low midband amplitudes and high slopes (Fig. 4).

The midband amplitude converged to the same mean value in porcine and equine samples (around 0.04 cm^{-1} sr^{-1} in Fig. 4a, b), though the BSC evolution was completely different in both cases. Conversely, the spectral slope allowed differentiation of the two species, indicating the different nature of RBC aggregation of each one.

A different kinetic behavior of the midband amplitude occurred in equine blood when using stabilization shears of 75, 50 and 25 s^{-1} (Fig. 4b). Contrary to the smooth increase observed in pig experiments, peaks of the midband amplitude appeared during the first 18 s of aggregation, then decreased to the same steady state as other shears. Spectral slope kinetics did not follow the same behavior.

Intra-assay variability of in vivo *measurements*

During the 10 repeated acquisitions on a volunteer, the median shear rate in the vein was stable with an average of 2.2 ± 0.6 s^{-1} (Fig. 5a). Note that only the low-flow technique was evaluated *in vivo*, as the stopped-flow approach lacked reproducibility *ex vivo*.

The spectral slope was repeatable with a coefficient of variation of 11% for the measures performed over 60 s (Fig. 5b). The midband amplitude exhibited the same stable kinetic, but presented more variability (coefficient of variation of 33%). Contrary to the *ex vivo* acquisitions, the erythrocyte aggregation did not exhibit an ascending kinetic during the first 60 s (exemplified by an increase in midband amplitude and a decrease in spectral slope).

Sensitivity of the ultrasound technique to biological inter-subject variations

A linear correlation (R^2 = 82.7%, p value < 0.0001) was found between the *ex vivo* index S_{10} and the spectral slope from *in vivo* acquisitions after 60 s of controlled flow (Fig. 6). It is noteworthy that the native hematocrit of participants was 46.6 ± 3.5% (range: 42%–52%). As mentioned earlier, it was adjusted to 40% for laser aggregometry measurements. The difference in hematocrit between *ex vivo* and *in vivo* results had little impact, as reflected by the good correlation nevertheless obtained. Also note that the two participants who disclosed pro-aggregating diseases (*i.e.,* aortic aneurysm and diabetes mellitus) scored the highest indexes with both techniques (Fig. 6).

The correlation between the index S_{10} and the midband amplitude was not significant (R^2 = 17.8%, p value = 0.21). The other laser aggregometry index S_{60} also exhibited a significant correlation with the spectral slope, although R^2

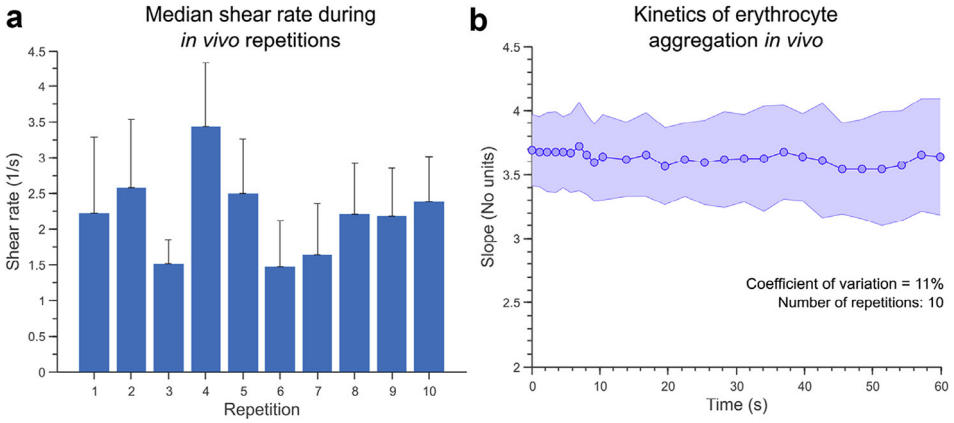

Fig. 5. (a) Evaluation of the control flow method during the ultrasound acquisitions *in vivo*. Each bar represents the average median shear rate during the 60 s of acquisitions for a single repetition. Measured median shear rate was close to the targeted value of 3 s^{-1}. (b) Aggregation kinetics monitored *in vivo* for 1 min using the spectral slope. The slope is quite stable during the whole ultrasound acquisition period.

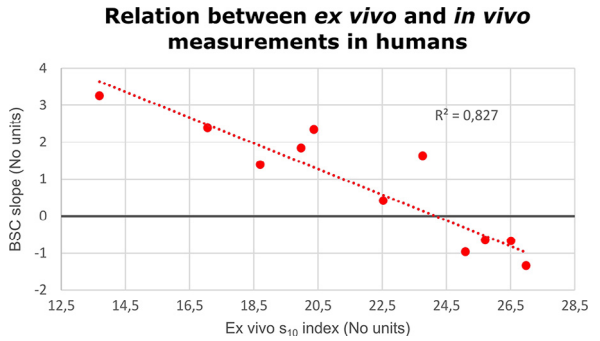

Fig. 6. Correlation between *ex vivo* index S_{10} and the backscatter coefficient spectral slope after 60 s of reduced flow *in vivo*. The *dark red points* represent two participants with chronic inflammatory conditions. They scored the highest values with both acoustic and laboratory techniques.

was lower than that with the index S_{10} (R^2 = 64.7%, p value = 0.001). The correlation between S_{60} and the midband amplitude was not significant (R^2 = 24.3%, p value = 0.103).

DISCUSSION

Techniques for controlling the flow shear rate

The low-flow technique for shear rate control permitted the distinction between different levels of RBC aggregation, both *in vivo* and *ex vivo*. This study is the first to report a correlation between *ex vivo* and *in vivo* measurements of erythrocyte aggregation in humans using ultrasound, which encourages future studies in patients with acute inflammatory conditions. The spectral slope parameter was more discriminating that the simple BSC amplitude at 25 MHz: in *ex vivo* experiments, porcine and equine samples shared the same midband amplitude and in *in vivo* experiments, this last parameter did not correlate well with laser aggregometry. However, overall results suggest that the raw BSC has distinguishable characteristics to allow differentiation of RBC aggregation levels.

Yet, the low-flow technique for *in vivo* measurements uses a different paradigm in two senses compared with *ex vivo* assessments. First, the *in vivo* technique employs a residual low shear rate that promotes a steady state of RBC aggregation after 1 min. The native shear rate before flow reduction and ultrasound acquisition is not easily controllable physiologically. On the contrary, the *ex vivo* technique uses the completely disaggregated state as starting point, followed by aggregate buildup after stopping the Couette rotation. Second, the proposed *in vivo* method employs a single measuring time point after the stabilization of the aggregation, instead of using the weighted sum of multiple points acquired during the aggregation kinetic, as done *ex vivo* by the laser aggregometer.

The method of simply stopping the flow with a tourniquet for *in vivo* applications is not optimum because of the lack of repeatability when the initial shear rate within the vein cannot be enhanced to disrupt RBC aggregates. The observed repeatability deficiency could be the result of the reduction of interaction between erythrocytes when the flow is abruptly stopped. Erythrocytes elongate while sheared, and when shearing stops, RBCs return to their normal shape, creating a cell-free layer around them (Dobbe et al. 2003). As the attraction force depends on inter-erythrocyte distances, some of the red cells would not have close neighbors to associate with (Shehada et al. 1993). Conversely, the application of a low shear rate, such as 3 or 5 s^{-1}, brings closer the erythrocytes and promotes their association, while not being high enough to completely dissociate already formed aggregates (Qin et al. 1998).

The similarity in the aggregation kinetics of porcine blood at 50 and 75 s^{-1} (Fig. 3a, c) suggests that the stopped flow could be repeatable if a complete disaggregation would be induced at the beginning of the acquisition. As introduced earlier, most commercial erythro-aggregometers use the complete disaggregation approach, driven by Couette or by plate-to-plate rheometry systems, to ensure repeatability (Baskurt et al. 2011). Some authors suggested the application of shakers over the vein to dissociate RBCs (Yu et al. 2005). However, there is no evidence that the disaggregation was complete in normal subjects participating in this study and that it could be effective in patients with enhanced RBC aggregation (*i.e.*, RBCs with stronger binding energy).

Clinical relevance of results

An intended aim of the ultrasound protocol is to propose an inflammatory marker for monitoring postoperative complications. Knowing the existence of a strong inflammatory reaction can help the clinician to guide its treatment. An appealing characteristic of the ultrasound method is that it can be implemented for continuous monitoring, in real time and at the bedside. On the contrary, laboratory tests of inflammation or of erythrocyte aggregation require blood sampling and at least 1 h for processing. Considering that a strong inflammatory reaction may occur during the first 2 h after a cardiopulmonary bypass surgery (Tripette et al. 2013), laboratory tests are thus not optimum in this context.

In addition, the proposed ultrasound technique can be used in other contexts requiring immediate assessment of the inflammatory condition. Examples of this include assessment of sepsis in emergency units (Reggiori et al. 2009), hyper-viscosity syndrome (Lacerda et al. 2017) and selection of graft donors (Avlonitis et al. 2005). Beyond inflammation detection, erythrocyte aggregation is also a

prognostic determinant of thrombus formation (Yu et al. 2011). In this context, the ultrasound protocol may allow the assessment of blood hyper-viscosity caused by high RBC aggregation, one of the factors of Virchow's triad of thromboembolism.

Behavior of the backscattering coefficient during the kinetic of RBC aggregation

A drawback of summarizing the backscattering coefficient with parameters is that this method hides some important characteristics of the frequency behavior of the BSC during RBC aggregation. Figure 7 illustrates *ex vivo* BSCs measured in Couette flow over a period of 120 s for the initial shear rate of 75 s^{-1}. In close to disaggregated states (t = 0 s), lower frequencies were less scattered than the higher ones, giving rise to a spectral slope close to 4, which is characteristic of Rayleigh scattering (see also Figs. 3c, d and 4c, d). This result has been observed several times in previous studies (Shung et al. 1976; Yu and Cloutier 2007). However, when some RBC aggregates were present, differences in scattering amplitude between low- and high-frequency ranges diminished, as evidenced by lower spectral slopes (Fig. 7b, d). Notably, in the highest aggregating conditions with horse blood, the slopes were close to zero (see the stabilization at 40 s in Fig. 4d), indicating a quasi-specular backscattering. Other researchers have observed the same behavior with whole blood (Foster et al. 1994; van der Heiden et al. 1995). However, parameterizing the BSC with single midband amplitude or spectral slope may be inappropriate under strong aggregation. Indeed, such conditions promote changes in the spectral slope over the measured bandwidth (*e.g.*, in Fig. 7b, d toward the end of the aggregation kinetics).

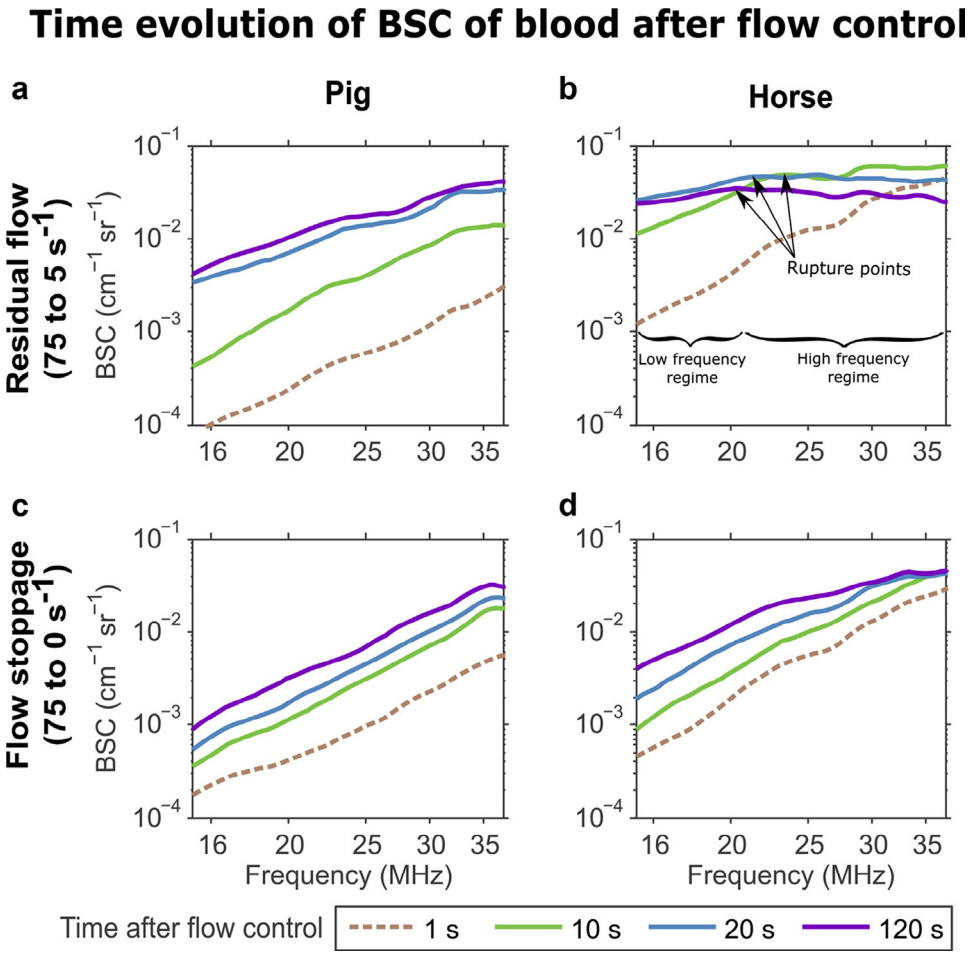

Fig. 7. Examples of erythrocyte aggregation kinetics *ex vivo* after flow control monitored by the frequency-dependent backscatter coefficient (BSC). Under disaggregated states (*dotted lines*), the spectral slope on a log-log scale is close to 4, indicating Rayleigh scattering. In the presence of erythrocyte aggregation, the spectral slope is reduced. With the biggest aggregates (panel b, horse blood at a low residual shear rate), the BSC presents two regions with characteristic slopes, named here the low- and high-frequency regimes; these regimes are separated by a characteristic rupture point, which is downshifted in frequency by stronger aggregation.

Rupture points between the low- and high-frequency regimes are typified in Figure 7b. Higher RBC aggregation promotes a shift of the rupture point toward lower frequencies. Thus, a better BSC parametrization would be necessary under these conditions.

In our study, the frequency behavior of the BSC was different from that predicted by recent blood scattering theories (de Monchy et al. 2016b; Franceschini et al. 2011). These theories predict that a collection of monodisperse scatterers produces constructive and destructive interference causing peaks and valleys in the BSC at characteristic frequencies. Non-aggregating RBCs theoretically produce frequency oscillations at frequencies above 100 MHz (Fontaine et al. 1999), whereas monodisperse aggregates downshift these oscillations toward lower frequencies (Franceschini et al. 2011). Earlier modeling also assuming monodisperse aggregates did not predict peak and valley frequency oscillations simply because the BSC was approximated by a second-order frequency-dependent Taylor expansion (Franceschini et al. 2008, 2010; Yu and Cloutier 2007). By considering polydispersity in RBC aggregate sizes (Fontaine and Cloutier 2003), simulations allowed observation of frequency-dependent backscatter with a single rupture point as in our current results.

On the basis of this discussion, it is clear that proper BSC modeling should consider the variability in RBC aggregate sizes (*i.e.*, their polydispersity). Instead of parametrizing the BSC with simple indices such as the midband amplitude and spectral slope, an alternative that would allow describing absence, normal and hyper-aggregating RBC conditions is to fit the BSC frequency response with a polydisperse effective medium theory considering the structure factor model, as recently proposed (de Monchy et al. 2016a). In this framework, the inverse problem allows assessment of the mean RBC aggregate size, their compactness and their size distribution (*i.e.*, polydispersity). Future work should focus on assessing the robustness of this BSC parametrization for *in vivo* measurements of RBC aggregation.

CONCLUSIONS

The flow shear rate is the main confounding factor for *in vivo* measurement of erythrocyte aggregation. Stopping the flow to nullify shearing forces is not an appropriate technique as the RBC aggregation level depends on the initial flow velocity within the vessel of interest. In contrast, the technique of acquiring the data with a low residual flow is repeatable and allows both *ex vivo* and *in vivo* detection of different levels of RBC aggregation. These results add more evidence supporting the feasibility and robustness of *in vivo* quantitative measurements of RBC aggregation with ultrasound. Because ultrasound is widely used, is low cost and is a point-of-care imaging method, the proposed technology could become an important tool in critical care medicine for monitoring the acute-phase inflammatory response (Tripette et al. 2013) and could also be of interest for predicting venous thrombotic events (Yu et al. 2011).

Acknowledgments—This work was financially supported by the Canadian Institutes of Health Research (grant #MOP-84358). Mr. Garcia-Duitama was recipient of a Ph.D. scholarship from the Fonds de recherche du Québec–Nature et technologies. Dr. Garcia received a research fellowship award from the Fonds de recherche du Québec–Santé. Authors want to thank Dr. Arnaud Louvet for his assistance during ultrasound acquisitions.

REFERENCES

Anderson JJ, Herd MT, King MR, Haak A, Hafez ZT, Song J, Oelze ML, Madsen EL, Zagzebski JA, O'Brien WD. Interlaboratory comparison of backscatter coefficient estimates for tissue-mimicking phantoms. Ultrason Imaging 2010;32:48–64.

Arwatz G, Smits A. A viscoelastic model of shear-induced hemolysis in laminar flow. Biorheology 2013;50:45–55.

Avlonitis VS, Wigfield CH, Kirby JA, Dark JH. The hemodynamic mechanisms of lung injury and systemic inflammatory response following brain death in the transplant donor. Am J Transplant 2005;5:684–693.

Baskurt OK, Meiselman H, Kayar E. Measurement of red blood cell aggregation in a "plate–plate" shearing system by analysis of light transmission. Clin Hemorheol Microcirc 1998;19:307–314.

Baskurt O, Boynard M, Cokelet G, Connes P, Cooke BM, Forconi S, Liao F, Hardeman M, Jung F, Meiselman H. New guidelines for hemorheological laboratory techniques. Clin Hemorheol Microcirc 2009;42:75–97.

Baskurt O, Neu B, Meiselman HJ. Red blood cell aggregation. Boca Raton, FL: CRC Press; 2011.

Berliner S, Rogowski O, Aharonov S, Mardi T, Tolshinsky T, Rozenblat M, Justo D, Deutsch V, Serov J, Shapira I. Erythrocyte adhesiveness/aggregation: A novel biomarker for the detection of low-grade internal inflammation in individuals with atherothrombotic risk factors and proven vascular disease. Am Heart J 2005;149:260–267.

Bigelow TA, O'Brien WD. Evaluation of the spectral fit algorithm as functions of frequency range and/spl delta/spl kappa/a/subeff/. IEEE Trans Ultrason Ferroelectr Freq Control 2005;52:2003–2010.

Bushberg JT, Leidholdt EM, Seibert AJ, Boone JM. Ultrasound imaging. In: The essential physics of medical imaging. Philadelphia: Lippincott Williams & Wilkins; 2002. p. 469–554.

Chien S, Usami S, Dellenback RJ, Gregersen MI, Nanninga LB, Guest MM. Blood viscosity: Influence of erythrocyte aggregation. Science 1967;157:829–831.

Cloutier G, Shung K. Study of red cell aggregation in pulsatile flow from ultrasonic Doppler power measurements. Biorheology 1992;30:443–461.

Cloutier G, Zimmer A, Yu FTH, Chiasson JL. Increased shear rate resistance and fastest kinetics of erythrocyte aggregation in diabetes measured with ultrasound. Diabetes Care 2008;31:1400–1402.

De Kroon M, Slager C, Gussenhoven WJ, Serruys P, Roelandt J, Bom N. Cyclic changes of blood echogenicity in high-frequency ultrasound. Ultrasound Med Biol 1991;17:723–728.

de Monchy R, Chayer B, Cloutier G, Franceschini E. Effective medium theory combined with a polydisperse structure factor model for characterizing red blood cell aggregation. Proc 2016 IEEE Int Ultrason Symp 2016;1–4. doi:10.1109/ULTSYM.2016.7728606.

de Monchy R, Destrempes F, Saha RK, Cloutier G, Franceschini E. Coherent and incoherent ultrasound backscatter from cell aggregates. J Acoust Soc Am 2016;140:2173–2184.

Destrempes F, Franceschini E, Yu FTH, Cloutier G. Unifying concepts of statistical and spectral quantitative ultrasound techniques. IEEE Trans Med Imaging 2016;35:488–500.

Dobbe JG, Streekstra GJ, Strackee J, Rutten MC, Stijnen JM, Grimbergen CA. Syllectometry: The effect of aggregometer geometry in the assessment of red blood cell shape recovery and aggregation. IEEE Trans Biomed Eng 2003;50:97–106.

Fåhraeus R. The suspension stability of the blood. Physiol Rev 1929; 9:241–274.

Fernandes CJ, Jr. The future has arrived. Crit Care Med 2013;41:2062–2063.

Fontaine I, Cloutier G. Modeling the frequency dependence (5–120 MHz) of ultrasound backscattering by red cell aggregates in shear flow at a normal hematocrit. J Acoust Soc Am 2003;113:2893.

Fontaine I, Bertrand M, Cloutier G. A system-based approach to modeling the ultrasound signal backscattered by red blood cells. Biophys J 1999;77:2387–2399.

Foster F, Obara H, Bloomfield T, Ryan L, Lockwood G. 1994 Ultrasound backscatter from blood in the 30 to 70 mhz frequency range. Proc 1994 IEEE Int Ultrason Symp 1994;1599–1602.

Franceschini E, Yu FTH, Cloutier G. Simultaneous estimation of attenuation and structure parameters of aggregated red blood cells from backscatter measurements. J Acoust Soc Am 2008;123:EL85–EL91.

Franceschini E, Yu FTH, Destrempes F, Cloutier G. Ultrasound characterization of red blood cell aggregation with intervening attenuating tissue-mimicking phantoms. J Acoust Soc Am 2010;127:1104–1115.

Franceschini E, Metzger B, Cloutier G. Forward problem study of an effective medium model for ultrasound blood characterization. IEEE Trans Ultrason Ferroelectr Freq Control 2011;58:2668–2679.

Franceschini E, Cloutier G. Modeling of ultrasound backscattering by aggregating red blood cells. In: Mamou J, Oelze ML (eds). Quantitative ultrasound in soft tissues. Dordrecht/Heilderlberg/New York/London: Springer; 2013. p. 117–145.

Garcia-Duitama J, Chayer B, Han A, Garcia D, Oelze ML, Cloutier G. Experimental application of ultrafast imaging to spectral tissue characterization. Ultrasound Med Biol 2015;41:2506–2519.

Garcia-Duitama J, Chayer B, Goussard Y, Cloutier G. 2016 Segmentation of blood layers with particle image velocimetry (PIV) for reproducible in vivo characterization of erythrocyte aggregation. Proc 2016 IEEE Int Ultrason Symp 2016;1–4. doi:10.1109/ULTSYM.2016.7728440.

Garcia DA. fast all-in-one method for automated post-processing of PIV data. Exp Fluids 2011;50:1247–1259.

Insana MF, Brown DG. Acoustic scattering theory applied to soft biological tissues. In: Shung KK, Thieme GA (eds). Ultrasonic scattering in biological tissues. Boca Raton, FL: CRC Press; 1993. p. 75–124.

Lacerda FH, de Mattos Mendes de Almeida VB, Nunes JT, de Carvalho Melo Júnior JA, Park M. Routine ultrasound-guided central venous access catheterization: A window to new findings! J Crit Care 2017;37:262–263.

Neumann FJ, Schmid-Schönbein H, Ohlenbusch H. Temperature-dependence of red cell aggregation. Pflügers Arch 1987;408:524–530.

Nguyen LC, Yu FTH, Cloutier G. Cyclic changes in blood echogenicity under pulsatile flow are frequency dependent. Ultrasound Med Biol 2008;34:664–673.

Qin Z, Durand L-G, Cloutier G. Kinetics of the "black hole" phenomenon in ultrasound backscattering measurements with red blood cell aggregation. Ultrasound Med Biol 1998;24:245–256.

Reggiori G, Occhipinti G, De Gasperi A, Vincent JL, Piagnerelli M. Early alterations of red blood cell rheology in critically ill patients. Crit Care Med 2009;37:3041–3046.

Rouffiac V, Guglielmi JP, Barbet A, Lassau N, Peronneau P. Application of validated ultrasound indices to investigate erythrocyte aggregation in pigs: Preliminary in vivo results. Ultrasound Med Biol 2004;30:35–44.

Scheipers U. Ultrasonic tissue characterization. In: Ukimura O, Gill I (eds). Contemporary interventional ultrasonography in urology. London: Springer London; 2009. p. 143–177.

Shehada R, Cobbold R, Mo L. Aggregation effects in whole blood: Influence of time and shear rate measured using ultrasound. Biorheology 1993;31:115–135.

Shung KK. On the ultrasound scattering from blood as a function of hematocrit. IEEE Trans Sonics Ultrason 1982;29:327–330.

Shung KK. Diagnostic ultrasound: Imaging and blood flow measurements. Boca Raton, FL: CRC Press; 2005. p. 185–202.

Shung KK, Sigelmann RA, Reid JM. Scattering of ultrasound by blood. IEEE Trans Biomed Eng 1976;460–467.

Tripette J, Denault AY, Allard L, Chayer B, Perrault LP, Cloutier G. Ultrasound monitoring of RBC aggregation as a real-time marker of the inflammatory response in a cardiopulmonary bypass swine model. Crit Care Med 2013;41:e171–e178.

Tripette J, Nguyen LC, Allard L, Robillard P, Soulez G, Cloutier G. In vivo venous assessment of red blood cell aggregate sizes in diabetic patients with a quantitative cellular ultrasound imaging method: Proof of concept. PloS One 2015;10:1–12.

van der Heiden MS, de Kroon MG, Bom N, Borst C. Ultrasound backscatter at 30 MHz from human blood: Influence of rouleau size affected by blood modification and shear rate. Ultrasound Med Biol 1995;21:817–826.

Wang SH, Shung KK. An approach for measuring ultrasonic backscattering from biological tissues with focused transducers. IEEE Trans Biomed Eng 1997;44:549–554.

Welch PD. The use of fast Fourier transform for the estimation of power spectra: A method based on time averaging over short, modified periodograms. IEEE Trans Audio Electroacoust 1967;15:70–73.

Weng X, Cloutier G, Beaulieu R, Roederer G. Influence of acute-phase proteins on erythrocyte aggregation. Am J Physiol Heart Circ Physiol 1996;271:H2346–H2352.

Weng X, Cloutier G, Pibarot P, Durand LG. Comparison and simulation of different levels of erythrocyte aggregation with pig, horse, sheep, calf, and normal human blood. Biorheology 1996;33:365–377.

Wertheim M. Exact solution of the Percus–Yevick integral equation for hard spheres. Phys Rev Lett 1963;10:321–323.

Windberger U, Bartholovitsch A, Plasenzotti R, Korak K, Heinze G. Whole blood viscosity, plasma viscosity and erythrocyte aggregation in nine mammalian species: Reference values and comparison of data. Exp Physiol 2003;88:431–440.

Yu FTH, Gennisson JL, Cloutier G. A new method to assess the kinetics of rouleaux formation in human subcutaneous veins using high frequency parametric imaging: Preliminary results. Proc 2005 IEEE Int Ultrason Symp 2005;870–873.

Yu FTH, Cloutier G. Experimental ultrasound characterization of red blood cell aggregation using the structure factor size estimator. J Acoust Soc Am 2007;122:645–656.

Yu FTH, Armstrong JK, Tripette J, Meiselman HJ, Cloutier G. A local increase in red blood cell aggregation can trigger deep vein thrombosis: Evidence based on quantitative cellular ultrasound imaging. J Thromb Haemost 2011;9:481–488.

Yuan Y, Shung K. Ultrasonic backscatter from flowing whole blood: I. Dependence on shear rate and hematocrit. J Acoust Soc Am 1988; 84:52–58.

Zhao H, Wang X, Stoltz J. Comparison of three optical methods to study erythrocyte aggregation. Clin Hemorheol Microcirc 1999;21: 297–302.